

The Research of Hydromechanics Methods with Changing Connectivity of the Mesh in Problems with Large Deformations

WANG Rui-li, LIN Zhong, LIN Wen-zhou

Abstract—A new automatic local remeshing method, based on changing the connectivity of meshes, is presented in this paper. When terminating computation in the Lagrangian framework is due to computational grids with large deformation problem, a remeshing phase in which a new grid is defined is introduced, with a remapping phase in which the Lagrangian solution is transferred (conservatively interpolated) onto the new grids. The new meshes after the remeshing phase is obtained so as to improve the mesh quality. If remeshing does not help improve the mesh, we present a new automatic local remeshing method, based on changing connectivity of the mesh, which to handle geometric intersection, and leads to general polygonal mesh. A series of numerical examples are presented to demonstrate the performance of our new method with the large deformation problems.

Index Terms—Automatic local remeshing, changing connectivity of the mesh geometric intersection, large deformation problem.

I. INTRODUCTION

In numerical simulation of multidimensional fluid flow, the relationship of the motion of the computational grid to the motion of the fluid is an important issue. There are two choices typically; one is Lagrangian framework, another is Eulerian framework. In the Lagrangian framework, the grid moves with the local fluid velocity, while in the Eulerian framework, the fluid flows through a grid fixed in space. Lagrangian framework is adopted in compressible fluid dynamics with multimaterial flows of high temperature and high pressure popularly. The Lagrangian methods have the natural advantage of well-resolved material interfaces, but the lagrangian meshes maybe distort in large deformation problems. The accuracy of the discrete scheme is reduced on the distorted grid, and the computation even run termination when the meshes distort too much. Therefore, the large

Manuscript received March 17, 2010. This work was supported by the national natural science foundation of china under Grant No. 90718029, the science foundation of laboratory of computational physics of china under Grant No. 9140C6902010903, and science foundation of CAEP (2009A0202014).

WANG Rui-li is with the Institute of Applied Physics and Computational Mathematics(IAPCM), Box 8009, Beijing, 100088 ; 0860-010-59872159 e-mail: wang_ruilii@iapcm.ac.cn .

LIN Zhong is with the Institute of Applied Physics and Computational Mathematics, Box 8009, Beijing, 100088 ; 0860-010-59872158 e-mail: lin_zhong@iapcm.ac.cn .

LIN Wen-zhou is with the Institute of Applied Physics and Computational Mathematics, Box 8009, Beijing, 100088 ; 0860-010-59872160 e-mail: lin_wenzhou@iapcm.ac.cn .

deformation problem is one difficulty and focus in Lagrangian methods, and the method to resolve the large deformation problem is the front field in computational fluids dynamic at present.

There are two reasons for the deformation of the Lagrangian methods: one is the un-robust of the numerical scheme, and the other is the grid evolution following the fluids. Thus robust scheme must be studied to make the Lagrangian method have strong adaptively, highly qualified grid.

In this paper we present a new automatic local remeshing method, based on changing connectivity of the mesh, which is used to handle geometric intersection problem. The first is an unstructured arbitrary polygonal mesh: the mesh is defined by a collection of control nodes that are topologically organized into cells. The mesh is unstructured in the sense that individual cells may be constructed from an arbitrary, non-uniform number of nodes. The second important aspect is allowed connectivity of the mesh to be changed (topology transformations) during the numerical simulation. Including topological operations such as splitting and elimination of cells and edges and merging of cells. This approach has successfully been implemented and is used in a number of 2D codes of numerical analysis.

II. POLYGONAL MESHES AND MOTIVATION

We consider a two-dimensional computational domain Ω , assumed to be a general polygon. We assume a mesh is given on Ω , whose cells, $\{c\}$, cover the domain without gaps or overlaps. Each cell may be a general polygon, and is assigned a unique index that for simplicity will also be denoted by c . The set of vertices (nodes) of the polygons is denoted by $\{n\}$, where each node has a unique index n . Then each cell can be defined by an ordered set of vertices. We denote the set of vertices of a particular cell c by $N(c)$. Further, we denote the set of cells that share a particular vertex n by $C(n)$. Note that each vertex may be shared by an arbitrary number of cells and we denote connectivity of the cell and node by $CNL(n)$ and $NCL(c)$. The connectivity of the cell $CNL(n)$ was be defined as an ordered set of nodes of around the cell, the connectivity of the node $NCL(c)$ was be defined as an ordered set of cells of sharing the node (see Fig. 1).

To motivate our research let us consider the problems with large deformations; quality of cells degrades and may become unacceptable for further calculation. Such as, in numerical simulation of multidimensional fluid flow, it is well known that the boundaries in the domain Ω

significantly changes and as time progresses, the boundaries

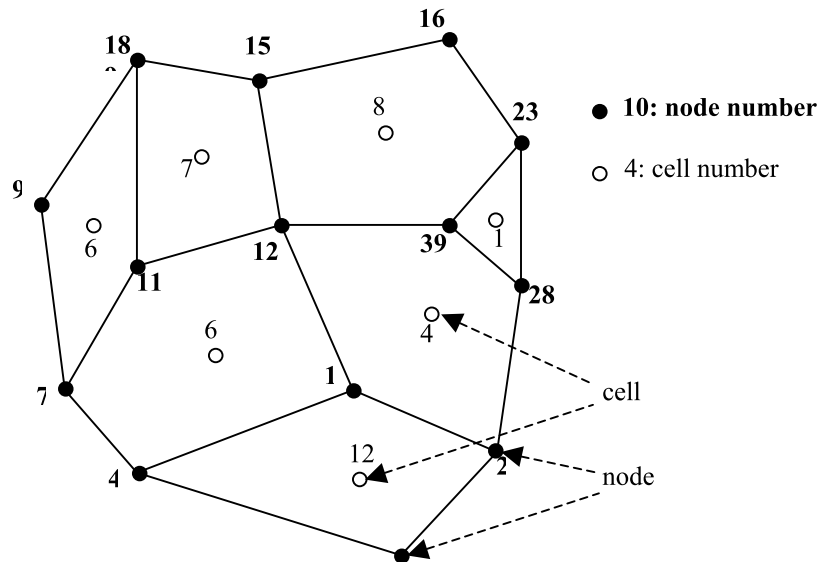


Fig.1 Polygonal mesh and notations. The set of nodes for cell $c=12$ is $CN(C=12)=\{5,2,1,4\}$, and the set of cells sharing node, $n=39$ is $NCL(n=39)=\{1,8,4\}$

may become necessary to topologically disconnect some of its regions or to remove singularities on the boundary. Here “singularities” means thin, wedge-shaped boundary cells, or intersection of cells and edges. If we allow connectivity of the mesh to change in unacceptable position which leads to general polygonal mesh. A quadrilateral cell can be local remeshing using topological operations such as elimination of cells and edges to triangles. This stage is described in Section 3.

III. TOPOLOGY TRANSFORMATIONS

These transformations include rearrangement of the local topology in order to arrive at a condition that will better admit a topology to form good elements. Some of these transformations have been described in other literature, but are described here for handling geometric intersection algorithm. Each of the following transformation have been implemented as part of this research, the basic transformation considered here are as follows.

A. Distinguishing intersection

A poor quality and unacceptable element need to pass topological operations. Firstly, its concave-point is distinguished using the vector product.

$$\begin{aligned} & (\mathbf{R}_{\alpha_j} - \mathbf{R}_{\alpha_{j-1}}) \times (\mathbf{R}_{\alpha_{j+1}} - \mathbf{R}_{\alpha_j}) \cdot \mathbf{k} \\ &= \left| \mathbf{R}_{\alpha_j} - \mathbf{R}_{\alpha_{j-1}} \right| \cdot \left| \mathbf{R}_{\alpha_{j+1}} - \mathbf{R}_{\alpha_j} \right| \sin \varphi \\ &= \begin{vmatrix} x_{\alpha_j} - x_{\alpha_{j-1}} & r_{\alpha_j} - r_{\alpha_{j-1}} & 0 \\ x_{\alpha_{j+1}} - x_{\alpha_j} & r_{\alpha_{j+1}} - r_{\alpha_j} & 0 \\ 0 & 0 & 1 \end{vmatrix} \\ &= (x_{\alpha_j} - x_{\alpha_{j-1}})(r_{\alpha_{j+1}} - r_{\alpha_j}) - (r_{\alpha_j} - r_{\alpha_{j-1}})(x_{\alpha_{j+1}} - x_{\alpha_j}) \end{aligned} \quad 3.1$$

Where \mathbf{k} denotes unit vector in θ -direction, in 3D space $(x-r-\theta)$, $\mathbf{k} = (0, 0, 1)^T$. φ is the angle between the

vector $(\mathbf{R}_{\alpha_j} - \mathbf{R}_{\alpha_{j-1}})$ and the vector $(\mathbf{R}_{\alpha_{j+1}} - \mathbf{R}_{\alpha_j})$.

If $(\mathbf{R}_{\alpha_j} - \mathbf{R}_{\alpha_{j-1}}) \times (\mathbf{R}_{\alpha_{j+1}} - \mathbf{R}_{\alpha_j}) \cdot \mathbf{k} < 0$, the node α_j is a concave-point in mesh- i . In Figure 2a the node α_j is a concave-point in mesh- i ; In Figure 2b the node α_j isn't a concave-point in mesh- i , it is a convex-point in mesh- i .

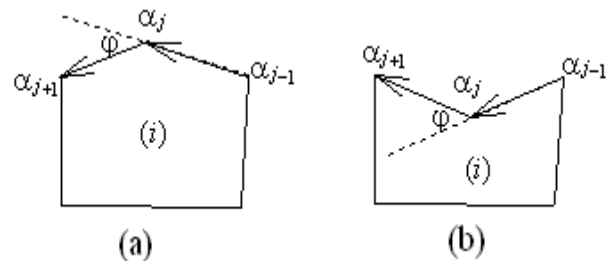


Fig. 2 concave-point and convex-point

Secondly, it is judged whether to intersect between any two non-adjacent segments of the element. In Figure 3, if following formula 3.2~3.5 is all satisfy, the line $\alpha_{j-1} \rightarrow \alpha_j$ and the line $\alpha_k \rightarrow \alpha_{k+1}$ have been intersected.

$$(\mathbf{R}_{\alpha_j} - \mathbf{R}_{\alpha_k}) \times (\mathbf{R}_{\alpha_{k+1}} - \mathbf{R}_{\alpha_k}) \cdot \mathbf{k} \geq 0 \quad 3.2$$

$$(\mathbf{R}_{\alpha_{j-1}} - \mathbf{R}_{\alpha_k}) \times (\mathbf{R}_{\alpha_{k+1}} - \mathbf{R}_{\alpha_k}) \cdot \mathbf{k} \leq 0 \quad 3.3$$

$$(\mathbf{R}_{\alpha_k} - \mathbf{R}_{\alpha_{j-1}}) \times (\mathbf{R}_{\alpha_j} - \mathbf{R}_{\alpha_{j-1}}) \cdot \mathbf{k} \geq 0 \quad 3.4$$

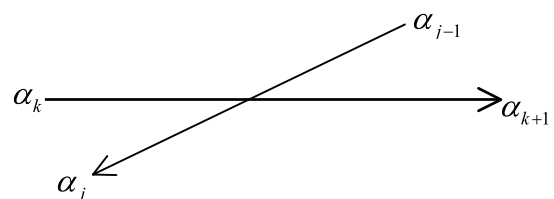


Fig. 3 intersections for two lines

$$\left(\mathbf{R}_{\alpha_{k+1}} - \mathbf{R}_{\alpha_{j-1}}\right) \times \left(\mathbf{R}_{\alpha_j} - \mathbf{R}_{\alpha_{j-1}}\right) \cdot \mathbf{k} \leq 0 \quad 3.5$$

We can base on concave-point in cell or intersection for two lines; it is very easy to distinguish intersection for fragment of the mesh in computing procedure. In Figure 4, the concave-point α_j at t^{n+1} cuts across the edge $\alpha_k \rightarrow \alpha_{k+1}$ in mesh- i , then the mesh- i becomes the intersection mesh. In this case, if any measure is not used during numerical simulation, it leads to reduce the accuracy of the discrete scheme or to terminate the computation.

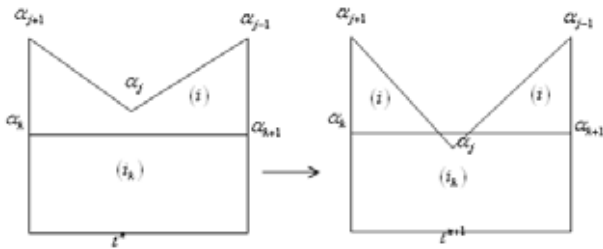


Fig. 4 intersection for two meshes

B. Changing connectivity of the mesh techniques

There is a very simple algorithm to handle intersection for fragment of the mesh. This problem can be resolved by using local changing connectivity of the mesh techniques “topological” remeshing. “topological” remeshing may be based on topological operations such as splitting and elimination of cells and edges and merging of cells optimization of poor topological quality mesh and further transformation of unacceptable cells into good cells. Here based on unstructured arbitrary polygonal meshes, connectivity of the mesh to change in numerical simulation are defined as lots of topological operations in our LAD2D code, such as cut down edge to mesh- i on the left, cut down edge to mesh- i on the right, big cut down edge to mesh- i on the left, big cut down edge to mesh- i on the right, merging or refining to mesh- i , fracture on the node, normal fracture on the common edge of two cells, and so on.

In Figure 5, when the node α_k is equal to the node α_{j+1} ($\alpha_k = \alpha_{j+1}$) of the mesh- i at t^{n+1} , the concave-point α_j cut across the edge $\alpha_k \rightarrow \alpha_{k+1}$ in mesh- i (only neighbor edge $\alpha_k \rightarrow \alpha_{k+1}$ with α_k), connectivity of the mesh- i to change, which to eliminate edge $\alpha_{j+1} \rightarrow \alpha_j$ of the mesh- i , is defined as cut down edge to mesh- i on the left. From this figure it is clear that topological is operation with logically quadrilateral element was changed triangles element.

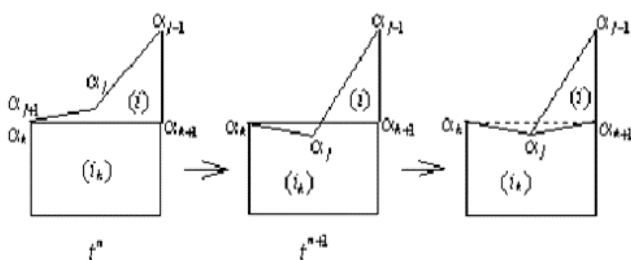


Fig. 5 cut down edge to mesh- i on the left

In Figure 6, when the node α_k is equal to the node α_{j+1} ($\alpha_k = \alpha_{j+1}$) of the mesh- i at t^{n+1} , the concave-point α_j cut across the edge $\alpha_k \rightarrow \alpha_{k+1}$ in mesh- i (the other neighbor edge $\alpha_k \rightarrow \alpha_{k+1}$ with α_k), connectivity of the mesh- i to change, which to eliminate edge $\alpha_{j+1} \rightarrow \alpha_j$ of the mesh- i , is defined as big cut down edge to mesh- i on the left.

In Figure 7, when the node α_{k+1} is equal to the node α_{j-1}

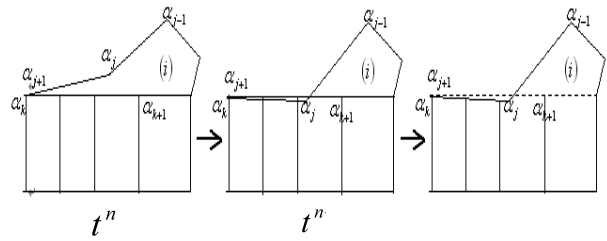


Fig. 6 big cut down edge to mesh- i on the left

($\alpha_{k+1} = \alpha_{j-1}$) of the mesh- i at t^{n+1} , the concave-point α_j cut across the edge $\alpha_k \rightarrow \alpha_{k+1}$ in mesh- i (only neighbor edge $\alpha_k \rightarrow \alpha_{k+1}$ with α_k), connectivity of the mesh- i to change, which to eliminate edge $\alpha_{j-1} \rightarrow \alpha_j$ of the mesh- i , is defined as cut down edge to mesh- i on the right.

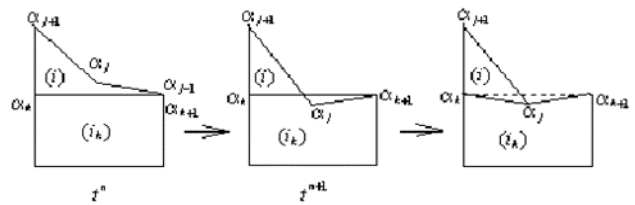


Fig. 7 cut down edge to mesh- i on the right

In Figure 8, when the concave-point α_j at t^{n+1} cut across the edge $\alpha_k \rightarrow \alpha_{k+1}$ in mesh- i , connectivity of the mesh- i to change, which to eliminate edge $\alpha_{k+1} \rightarrow \alpha_k$ of the mesh- i , is defined as merging to mesh- i , and which to refine edge $\alpha_{k+1} \rightarrow \alpha_k$ of the mesh- i , is defined as refining to mesh- i .

The proposed method of automatic local remeshing is implemented as a dynamic link library. In case of remeshing, the calling program receives information on all removed, changed and new nodes and cells and also on intersections of new and old cells which are needed for rezoning.

After topological operations Lagrangian solution is transferred conservatively interpolated from some polygonal meshes to another.

IV. NUMERICAL TESTS

In this section, we present the numerical results obtained from the Lagrangian adaptive hydrodynamics code in 2-D

space (LAD2D)[2]. LAD2D is a software project based on an explicit Lagrangian finite difference scheme with models

The equation of state of gas is used with $p = (\gamma - 1)\rho e$, the

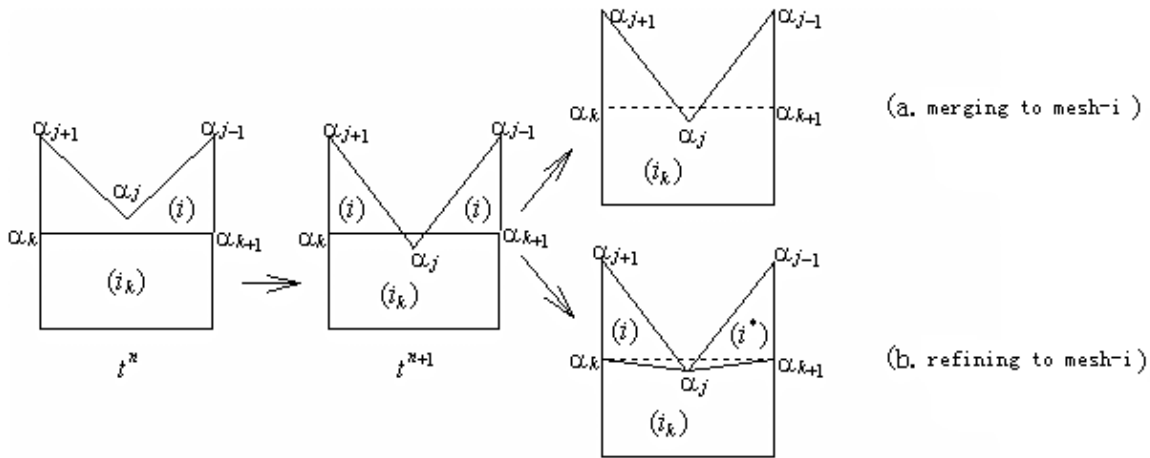


Fig. 8 merging or refining to mesh-i

of elasto-plasticity, material damage and detonation, using the above method.

The first test is the simple test case in planar geometry, and separates the air-region in the computational process. Most of the methods was not natural simulated this problem. The second is a “Diffraction of a detonation wave behind a backward-facing step” problem in r-z-axisymmetric geometry. It is often numerical simulation in order to validate the predictive capabilities of the new method-we compare numerical results with experimental data.

A. The simple test case

Let’s consider the simple problem with breaking of region in planar geometry. This problem is a two layers material problem. The computational domain is $\Omega = [0; 1.0] \times [0; 0.12]$ as described in figure 9. The lower layer is a ideal gas, The gas-region is $\Omega_1^{air} = [0; 1.0] \times [0; 0.1]$, The upper layer is a iron-metal(Fe), The region is $\Omega_2^{Fe} = [0; 1.0] \times [0.1; 0.12]$, the initial densities are $\rho_1 = 0.0129$, $\rho_2 = 7.85$, the initial pressures are $p_1 = 0.1$, $p_2 = 1.0$, the initial velocity is zero in gas-region, the initial velocity is a distribution in the Fe-region as described by formula :

$$\begin{cases} u = 0.0 \\ v = 20.0 * \sqrt{(x - 0.1)^2 + (y - 0.1)^2} \end{cases} \text{ if } 0.1 < x \leq 0.5$$

$$\begin{cases} u = 0.0 \\ v = 20.0 * \sqrt{(0.9 - x)^2 + (y - 0.1)^2} \end{cases} \text{ if } 0.5 \leq x < 0.9$$

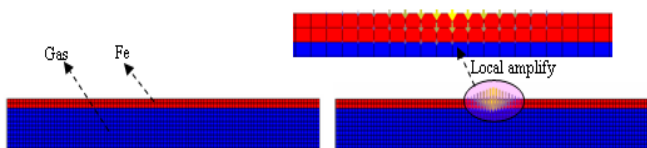


Fig. 9 Schematics and meshes and initial condition of model

adiabatic constant $\gamma = 1.4$. The equation of state of iron-metal(Fe) is used with $p = (\gamma - 1)\rho e + c_0^2(\rho - \rho_0)$.

Where $\gamma = 4.075$ $c_0 = 4.2 \text{ km/s}$

Figure 10 shows the process of automatic separating in gas layer. Begins iron-metal is getting fell until it meet the boundary of gas, then the gas region is separated into two parts using automatic local remeshing techniques. From the figures it is clear that the connectivity of the mesh is changed.

B. Diffraction of a detonation wave behind a backward-facing step

Diffraction of a detonation wave behind a backward-facing step is one of the fundamental topics in shock wave dynamics and is studied extensively by many researchers. Here It is numerical simulation in order to validate the predictive capabilities of the new automatic local remeshing method, based on Lagrangian methods, for problems with large deformations.

This problem models is a detonation wave propagating through the channels with suddenly expending section. The left is a little section channels, the right region is a large section channels. Initially, the region between the inlet and the end of the reaction zone is taken to be at the CJ state. The walls of the channel are held rigid, and a no-reflection boundary condition is applied at the outlet. The computational domain is Ω as described in figure 11. Ω is split into two regions filled with the explosive PBX9404 with parameters $K=2.996$, $D_j=8.88 \text{ km/s}$, $\rho_0=1.84 \text{ g/cm}^3$. The left region is $\Omega_1 = [0; 3.0] \times [0; 0.5]$, The right region is $\Omega_2 = [3.0; 6.0] \times [0; 3.0]$. The driver section is in the left part of the Ω_1 , the top boundary condition is a rigid; the bottom boundary condition is a axially symmetric.

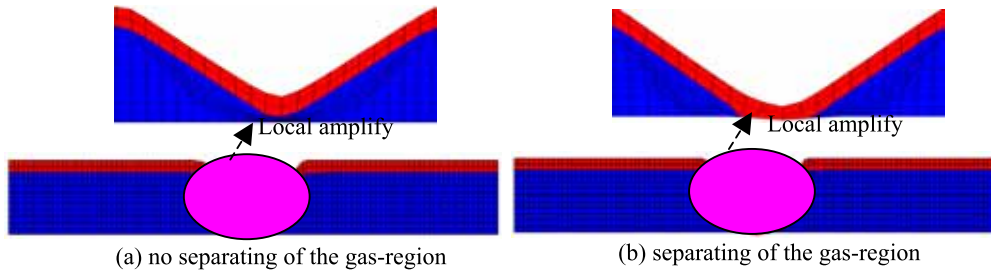


Fig. 10 the process of automatic separating in gas layer

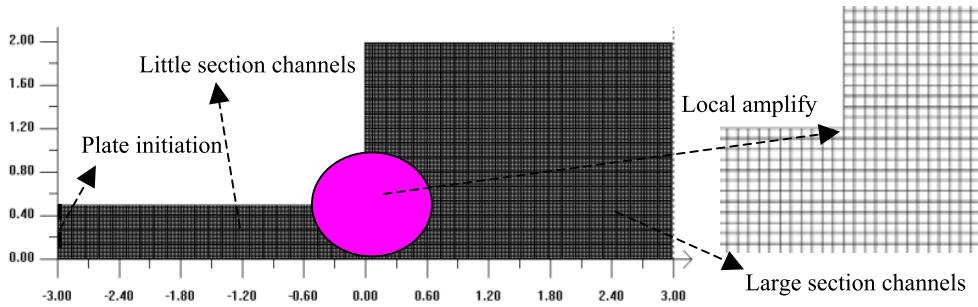


Fig. 11 The computing model and initial meshes

● Reaction rate function

In numerical simulation of detonation, combustion function F means the extent of explosive reaction. Three zones are distinctly distinguished (see Figure 12).

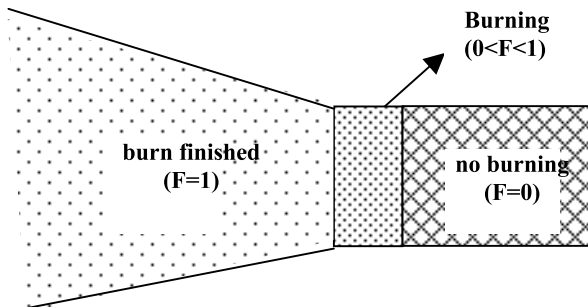


Fig. 12 Process of explosive reaction with combustion function F

Combustion function F is $F = [\max(F_1, F_2)]^{n_b}$,

where Wilkins function F_1 is

$$F_1 = \begin{cases} 0, & \text{no burning} \\ (1-V)/(1-V_j), & \text{burning} \\ 1, & \text{burn finished} \end{cases}$$

C-J burn function F_2 is

$$F_2 = \begin{cases} 0, & t \leq t_b \\ (t-t_b)/\Delta L, & t_b < t < t_b + \Delta L \\ 1, & t \geq t_b + \Delta L \end{cases}$$

Where $V_j = \gamma/(\gamma-1)$ denotes specific volume; t is current time; t_b is the burn-beginning time; $\Delta L = r_b \Delta R / D_j$, ΔR is cell width; D_j is the constant speed of propagation of the front; n_b, r_b are adjustable parameters.

● Equation of state

The equation of state of the explosive is used with the Jones-Wilkins-Lee JWL :

$$p = A \exp(-R_1 V) + B \exp(-R_2 V) + \frac{\omega E}{V}$$

Where $V = \rho_0 / \rho$, $E = \rho_0 e$, the JWL equation of state parameters for the non-reacted explosives and their reaction products are used with $A = 852.4 GPa$, $B = 18.02 GPa$, $R_1 = 4.6$, $R_2 = 1.3$, $w = 0.38$.

● Results and discussion

The first, a steady CJ detonation wave propagates through the narrow segment unit diffraction around a 90° corner, begins its travel through the narrow channel as a steady, undisturbed wave. It first senses a change in geometry upon arriving at the corner. As the detonation wave rounds the corner, the diffraction and re-initiation of detonations behind a backward-facing step generated spherical detonation wave. The detonation wave is weakened to deflagration partly in initial the large section channels according to detonation wave diffraction. The slip line could be formed, and the Mach reflection of detonation wave had occurred when the detonation wave interact with the wall. As time elapses, near the line of symmetry (bottom boundary of the computational domain) was reflected wave interacts with the back-face of the step where a vortex exists, the wave becomes planar and the reflection on the wall transits to a Mach reflection and the reflected wave reflects off the upper wall again. Figure 13 shows the mesh in the 90° corner. From this figure it is clear that topological is operation with logically quadrilateral element was changed triangles element. The mesh is so high deformation in near the corner that pure Lagrangian schemes eventually fail.

Figure 14 shows the computing mesh (upper) and density contours (lower) at three times. Diffraction through the

90° corner also generates a stronger corner vortex. We compare numerical results with experimental data by using high-speed schlieren photography[6], which conforms qualitatively.

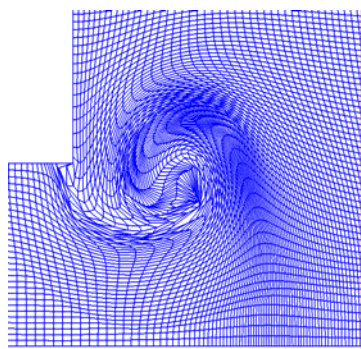


Fig.13 Meshes in a time during numerical simulation

V. CONCLUSIONS

We have presented a new automatic local remeshing method, based on changing connectivity of the mesh. It includes two main elements.

An unstructured arbitrary polygonal mesh system is defined, and a Lagrangian phase with finite volume methods in which the solution on polygonal mesh is updated.

The automatic local remeshing method is defined using topology transformations techniques. It allows the change of

mesh connectivity, and Lagrangian solution is transferred (conservatively interpolated) from some polygonal meshes to another.

A series of numerical examples is presented to demonstrate the robustness of our method is robust in large deformation problems, and show the predictive capabilities of the new automatic local remeshing method.

We recognize that our new method requires more testing, which is the remaining work in the future.

REFERENCES

- [1] D.J. Benson, Computational methods in Lagrangian and Eulerian hydrocodes, *Comp. Meth. Appl. Mech. Engrg.*, 99, 235-394, 1992.
- [2] WANG Rui-li, LIN Zhong, NI Guo-xi, Base on arbitrary N-polygon Lagrange grids finite volume method and applications. *Journal on numerical methods and computer applications*, 2006, 27(1): 31-38. (in Chinese)
- [3] J.C. Campbell, M.J. Shashkov, A Compatible Lagrangian Hydrodynamics Algorithm for Unstructured Grids. *Selcuk J. Appl. Math.*, 4(2): 53-70, 2003.
- [4] P. Knupp, L.G. Margolin, and M. Shashkov, Reference Jacobin optimization-based rezoned strategies for arbitrary lagrangian eulerian methods. *J. Comput. Phys.* 176: 93-128, 2002.
- [5] DU Yang, SHEN Wei, ZHOU Jian-zhong, Numerical simulation of detonation wave propagating through the channels with suddenly expanding section [J]. *explosion and shock waves*, 2004 24 1 75-79. (in Chinese)
- [6] S. Ohyagi, T. Obara, S. Hoshi, P. Cai, T. Yoshihashi, Diffraction and re-initiation of detonations behind a backward-facing step. *Proceedings of the 18th Int. Colloquium on the Dynamics of explosions and reactive systems at Seattle, USA, 2002.*

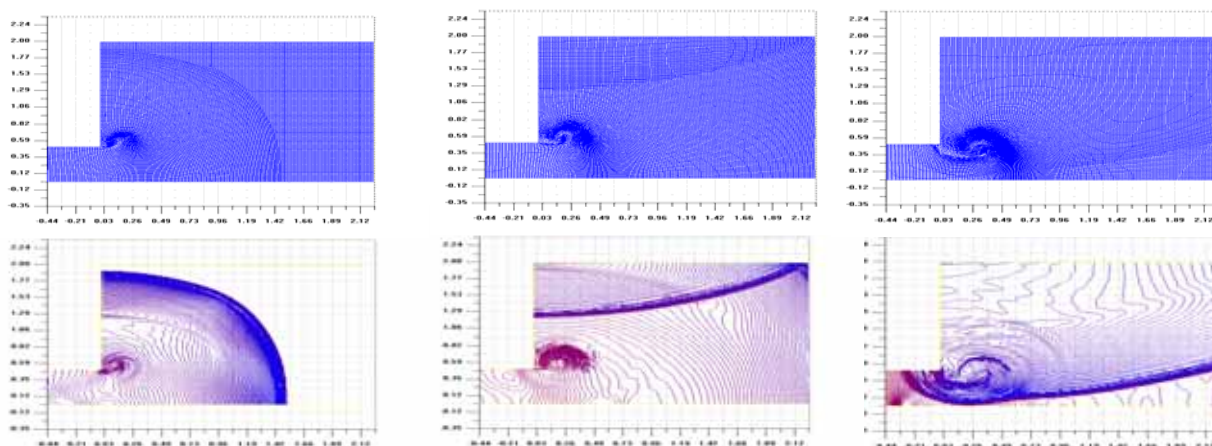


Fig. 14 The computing mesh (upper) and density contours (lower)